Intermolecular Interaction in Multicomponent Supramolecular Complexes through Hydrogen-Bonding Association

Jianwei Xu,[†] Chaobin He,*[,†] Kee Chua Toh,[†] and Xuehong Lu[‡]

Institute of Materials Research and Engineering, 3 Research Link, Republic of Singapore, Singapore 117602, and School of Materials Engineering, Nanyang Technological University, Republic of Singapore, Singapore 639798

Received June 21, 2002; Revised Manuscript Received September 4, 2002

ABSTRACT: A series of main-chain hydrogen-bonded supramolecular complexes have been prepared by self-assembly of proton donor (diacid) and acceptor (bipyridyl ethylene) through the formation of intermolecular hydrogen bonds. The phase transition behaviors were studied using differential scanning calorimetry and polarized optical microscopy. X-ray photoelectron spectroscopy study indicated that the binding energy of N 1s upshifted ca. 0.8 eV, which was within the limit of the hydrogen-bonding interaction. Solid-state CP/MAS ^{13}C NMR spectroscopy experiments revealed that an induced upfield shift ($\Delta\delta \geq 4$ ppm) of carbonyl carbon in solid state was observed as a result of the formation of intermolecular hydrogen bond. The natural abundance CP/MAS ^{15}N NMR spectroscopy also supported that the molecular complexes with hydrogen bond characteristics rather than zwitterionic complexes were formed on the basis of the change in ^{15}N chemical shift.

Introduction

Hydrogen bonding is the most important noncovalent interaction in chemistry and biological system. It plays a key role in the assembly of molecules to generate supramolecular hydrogen-bonded liquid crystals.[1−12] The hydrogen bonding induces the molecule assembly and thus results in the formation of liquid crystallinity. The hydrogen-bonded liquid crystals can be synthesized using two different components, proton donor (D) and proton acceptor (A), through complementary assembly. The hydrogen bond acts as a linkage to hold the two rigid components together and thus form a mesogenic phase. If the two components possess bifunctional groups, for example, diacid and bibyridyl derivative, a liquid crystalline polymer will be formed by extending the D−A interaction.[13−16] Many methods can be used to investigate the hydrogen-bonded liquid crystals. For example, Fourier transformation infrared (FT-IR) is a useful technique in interpreting the D−A interaction as the hydrogen bond is sensitive to temperature and distinguishable from the donor associate and D−A associate in the IR absorption. Differential scanning calorimetry (DSC) is another common method to study the thermal properties of liquid crystals. The interaction between D and A can give rise to two different bonding modes, i.e., the hydrogen bonding and ionic bonding. It is, however, that both FT-IR and DSC are not sensitive in probing the nature of the D−A interaction. Moreover, there is still a controversy of which the bonding mode is dominated in the D−A interaction. The hydrogen bond energy (2−10 kcal mol^{-1}) is much less than the covalent bond energy (35−135 kcal mol^{-1}), but the formation of the hydrogen bond does result in a change of electron density of relevant nuclei although it is subtle. Nuclear magnetic resonance (NMR) spectroscopy[17−20] and X-ray photoelectron spectroscopy (XPS)[21−25] are good tools to explore the D−A interaction. In this work we prepare a series of binary and ternary supramolecular complexes by using the melting method. These complexes are studied by DSC, polarizing optical microscopy (POM), solid-state CP/MAS ^{13}C NMR, CP/MAS ^{15}N NMR, and XPS. In addition, the third bifunctional component, which serves as the second proton donor, is incorporated into the complexes and will to some extent govern the properties of the liquid crystalline polymers. It is expected that, through this research, the nature of the D−A interaction, in particular either the hydrogen-bonding interaction or ionic interaction, can be elucidated.

Scheme 1

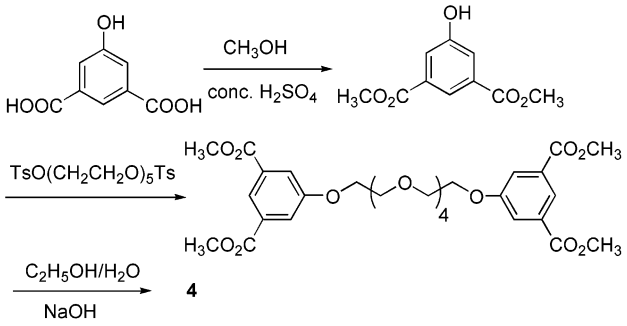

4

Experimental Section

Materials. 1,14-Bis(4′-carboxyphenoxy)-3,6,9,12-tetraoxatetradecane (**1**), 1,11-bis(4′-carboxyphenoxy)-3,6,9-trioxaundecane (**2**), and 1,8-bis(4′-carboxyphenoxy)-3,6-dioxaoctane (**3**) were synthesized by reaction of methyl *p*-hydroxybenzoate with oligoethylene glycol ditosylate, followed by hydrolysis in aqueous NaOH/ethanol. The spectroscopic data of compounds **1**−**3** are consistent with the authentic samples. 1,14-Bis(3′,5′-dicarboxyphenoxy)-3,6,9,12-tetraoxatetradecane (**4**) was prepared by reaction of 5-hydroxyisophthalic acid dimethyl ester with pentaethylene glycol ditosylate, followed by hydrolysis with aqueous NaOH/ ethanol as shown in Scheme 1. ^{1}H NMR (300 MHz) δ [dimethyl sulfoxide (DMSO-d_6), ppm]: 8.11 (s, 2H), 7.67 (s, 4H), 4.24 (m, 4H), 3.80 (m, 4H), 3.62 (m, 4H), 3.56 (m, 4H), 3.54 (m, 8H). ^{13}C NMR δ [DMSO-d_6, ppm]:

[†] Institute of Materials Research and Engineering.
[‡] Nanyang Technological University.
* To whom correspondence should be addressed: Tel 65-6874-8145; Fax 65-6872-7528; e-mail cb-he@imre.org.sg.

10.1021/ma020971u CCC: $22.00
Published on Web 10/04/2002

Table 1. Thermal Behaviors of Supramolecular Complexes[a]

	phase transition behaviors			
complex	1st heating	2nd heating	1st cooling	2nd cooling
1/6	K 165 I	K 159 I	I 156 N 133 K	I 156 N 132 K
$\mathbf{1}_{0.9}/\mathbf{5}_{0.1}/\mathbf{6}$	K 165 I	K 157 I	I 159 N 112 K	I 159 N 112 K
$\mathbf{1}_{0.75}/\mathbf{5}_{0.25}/\mathbf{6}$	K 156 I	K 156 I	I 163 N 125 K	I 162 N 125 K
2/6	K 178 I	K 177 I	I 174 N 154 K	I 173 N 153 K
$\mathbf{2}_{0.9}/\mathbf{5}_{0.1}/\mathbf{6}$	K 175 I	K 173 I	I 176 N 135 K	I 175 N 132 K
$\mathbf{2}_{0.75}/\mathbf{5}_{0.25}/\mathbf{6}$	K 173 I	K 172 I	I 181 N 127 K	I 180 N 125 K
3/6	K 215 I	K 214 I	K 205 I	K 203 I

[a] Transition temperature (°C). K = crystalline, N = nematic, and I = isotropic. Heating and cooling rates were 10 °C min^{-1}. Transition temperatures were taken at the maximum of transition peaks.

167.25, 159.48, 133.46, 123.18, 120.00, 70.81, 70.64, 69,64, 68.66. IR (KBr): 3448 (O−H), 1707 cm^{-1} (C═O). 4,4′-Oxybis-(benzoic acid) (**5**) was purchased from Aldrich and used as received. *trans*-1,2-(4-Pyridyl)ethylene (**6**) was purchased from Aldrich and recrystallized three times from ethyl ethanoate and *n*-hexane before use.

Supramolecular complexes were prepared by mixing a stoichiometric amount of proton donor (diacid or tetraacid) and proton acceptor (**6**). The mixture was heated with magnetic stirring to ca. 200 °C until all solids are melted to form a transparent liquid. The liquid was kept for 1 min at this temperature and then allowed to cool to room temperature in air for analysis.

Instrumentation. Solution NMR spectra were acquired on a Bruker ACF (300 MHz) NMR spectrometer. TMS is used as an internal reference. The solid-state ^{13}C and ^{15}N NMR spectra were measured by the cross-polarization method on a Bruker DRX-400 NMR spectrometer at 298 K with a Bruker CP/MAS probe. A 7 mm rotor of zirconium oxide and a spinning frequency of 5.5 kHz (or 4 kHz) were used for all CP/MAS experiments. For solid-state ^{13}C NMR, an 8 μs 90° pulse length, a 2 ms contact time for cross-polarization, and a 33 ms acquisition time with the cycle delay of 3 s were used. ^{13}C chemical shifts were referenced to an external standard of adamantane, methylene resonance at 38.56 ppm relative to TMS. For solid-state ^{15}N NMR, a 10 μs pulse length, a 3 ms contact time, and a 50 ms acquisition with the cycle delay of 10 s were used. ^{15}N chemical shifts were referenced to an external standard of (98% ^{15}N-labeled)-glycine at 341.84 ppm relative to TMS. XPS measurements were carried out on an ESCALAB 220i-XL spectrometer using a Mg Kα X-ray source (1253.6 eV). The X-ray source was run at 12 kV and 10 mA. All core-level spectra were referenced to the C 1s neutral carbon peak at a binding energy of 285.0 eV in order to compensate for surface charge effects. The pressure in the analysis chamber was maintained under ultrahigh vacuum at 10^{-9} mbar. Differential scanning calorimetry experiments were carried out on a TA Instrument DSC 2920 at a heating rate of 10 °C min^{-1} in nitrogen. Photomicrographs were taken on a Nikon OPTIPHOT2-POL polarizing optical microscope, equipped with a TMC-6RGB1/2" color CCD camera and a temperature programmer TP-93.

Results and Discussion

DSC and POM Study. The structures of the proton acceptor and donors used in this paper are shown in Scheme 2. All compounds in our study are nonmesogenic. The supramolecular complexes were analyzed by DSC and POM. The thermal properties of complexes are summarized in Table 1. The DSC curves of complexes **1/6,** $\mathbf{1}_{0.9}/\mathbf{5}_{0.1}/\mathbf{6}$, and $\mathbf{1}_{0.75}/\mathbf{5}_{0.25}/\mathbf{6}$, as examples, are also given in Figure 1. For **1**-containing complexes, the melting temperature of complexes slightly decreased with the increase of **5** content on the second heating, but the isotropic−nematic transition temperature increased with the addition of **5** on the first and second cooling. Surprisingly, the crystallization temperature does not constantly correlate to the relative content of **5** on the first and second cooling. For **2**-containing complexes, the melting temperature followed the same trend as the **1**-containing complexes on the second heating, and the isotropic−nematic transition temperature increases with the increase of **5** content. Unlike the **1**-containing complexes, the crystallization temper-

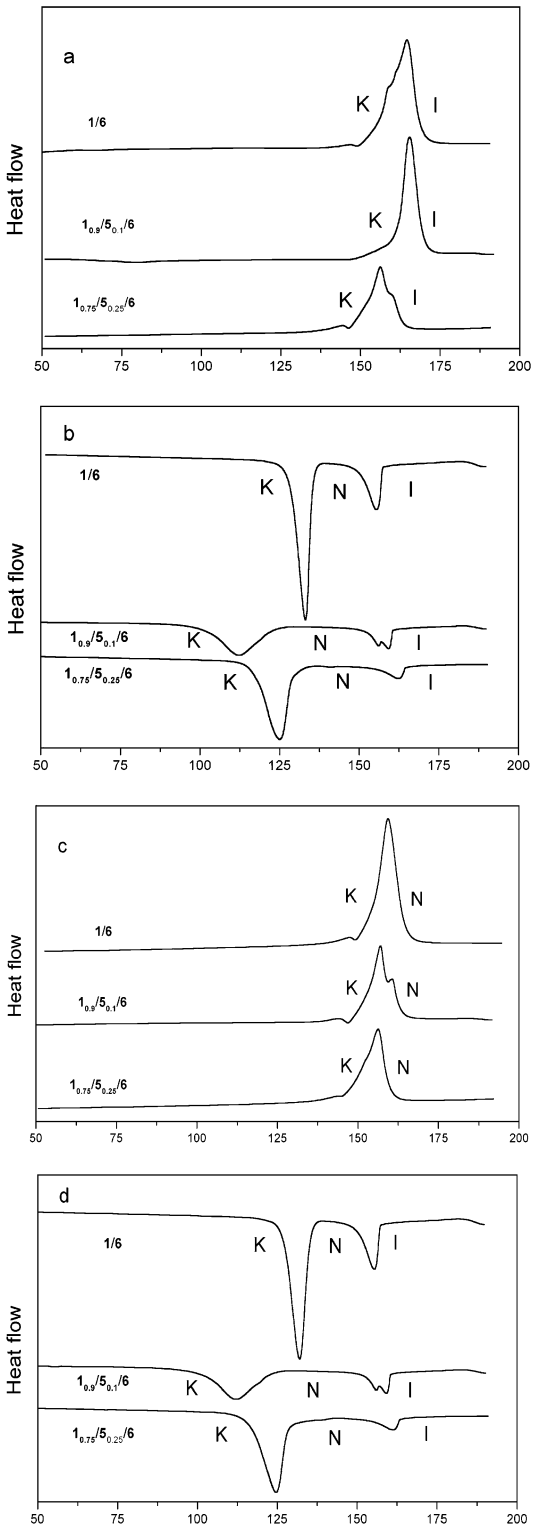

Figure 1. DSC curves of complexes **1/6,** $\mathbf{1}_{0.9}/\mathbf{5}_{0.1}/\mathbf{6}$, and $\mathbf{1}_{0.75}/\mathbf{5}_{0.25}/\mathbf{6}$: (a) the first heating, (b) the first cooling, (c) the second heating, and (d) the second cooling.

Scheme 2. Structures of Hydrogen Bond Donor, Acceptor, and Supramolecular Complexes

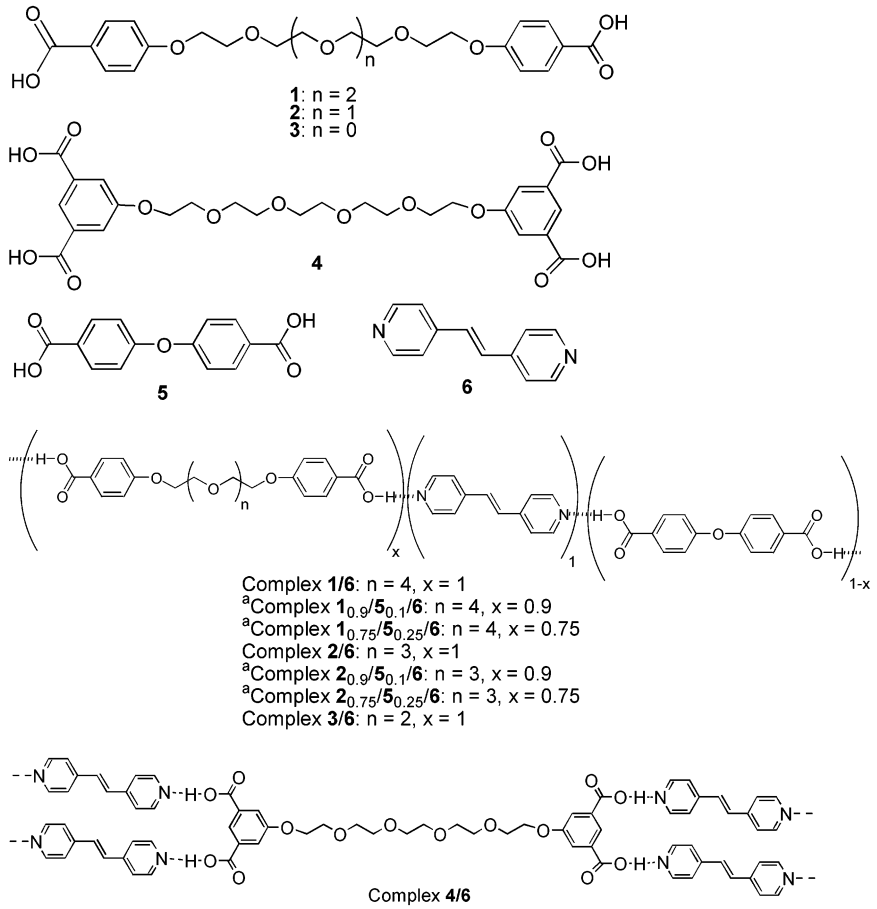

[a] Subscript denotes the molar fraction of the donor component in the complexes.

ature decreases with the increase of **5** content on the first and second cooling. Addition of **5** has a twofold effect on the thermal properties of complexes. First, incorporation of **5** causes a random chain structure that does not favor crystallization. Second, the kink conformation of **5** also retards the crystallization. As a result, the melting temperature decreases as **5** content increases. On the other hand, the increase of the isotropic−nematic transition temperature for the complexes could be attributed to the rigidity of **5** that prefers to a more stable mesophase. All complexes exhibited liquid crystallinity except for complex **3/6**. Since **3** consists of a relative shorter flexible polyether chain than compounds **1** and **2**, it may reduce flexibility of the polymer chain formed, and thus produce the higher crystallization temperature than the mesogenic phase transition temperature, and subsequently lose its liquid crystal property. Complex **4/6** was also examined by POM; however, no mesogenic phase was observed upon cooling or heating. Compound **4** has four proton-donating groups so as to readily form a cross-linked hydrogen-bonded polymer. Although it has been reported that multifunctional proton donors and bipyridyl derivatives formed supramolecular liquid crystals,[11,12,26] in our case only a glassy state was observed for **4/6**. It is likely to form a higher degree of networked polymer with higher relative molecular mass so that **4/6** does not exhibit a mesogenic phase.

Complexes **1**$_{0.9}$/**5**$_{0.1}$/**6**, **1**$_{0.75}$/**5**$_{0.25}$/**6**, **2**$_{0.9}$/**5**$_{0.1}$/**6**, and **2**$_{0.75}$/**5**$_{0.25}$/**6** exhibited a nematic phase. Polarizing optical micrographs of complexes **1**$_{0.9}$/**5**$_{0.1}$/**6**, **1**$_{0.75}$/**5**$_{0.25}$/**6**, **2**$_{0.9}$/**5**$_{0.1}$/**6** and **2**$_{0.75}$/**5**$_{0.25}$/**6** are shown in Figure 2. The homotropic textures of the nematic phase are observed for complexes **1**$_{0.9}$/**5**$_{0.1}$/**6** and **1**$_{0.75}$/**5**$_{0.25}$/**6** at 165 and 166 °C, respectively, upon cooling. In contrast, the Schlieren textures of the nematic phase are seen for complexes **2**$_{0.9}$/**5**$_{0.1}$/**6** and **2**$_{0.75}$/**5**$_{0.25}$/**6** at 193 and 190 °C, respectively, upon cooling. The complex **1**$_{0.9}$ /**5**$_{0.1}$/**6** exhibited a nematic phase on the first cooling and subsequent both heating and cooling. It differs from **1**/**6**, which showed an enantiotropic smectic A phase on the second and subsequent heating. Complex **1**$_{0.9}$ /**5**$_{0.1}$/**6** in fact kept a reversible dynamic equilibrium (isotropic ⇔ nematic ⇔ isotropic) within a very short temperature range (166−164 °C). Like complexes **1**$_{0.9}$ /**5**$_{0.1}$/**6**, the complex **1**$_{0.75}$/**5**$_{0.25}$/**6** exhibited a nematic phase on cooling. If the relative content of donor **5** increases by 50% of molar fraction, the complexes did not form a liquid crystal. Complex **2**/**6** formed a monotropic smectic A phase,[27,28] but complexes **2**$_{0.9}$/**5**$_{0.1}$/**6** and **2**$_{0.75}$/**5**$_{0.25}$/**6** just demonstrated a monotropic nematic phase upon cooling. It is well-known that the nematic phase is a mesophase that possesses the lowest structure order. The molecules in the nematic phase are arranged less ordered than that in the smectic phase. Addition of the second rigid donor **5** may reduce the order of complementary assembly and subsequently makes ternary complexes merely exhibit less ordered nematic phase.

XPS Characterization. The XPS technique is useful to study the noncovalent interaction, especially for the hydrogen-bonding and ionic interaction, in the polymer bends and complexes.[21−25] The formation of the hydrogen bond between the donor and acceptor would change the chemical environment. The hydrogen bonding makes

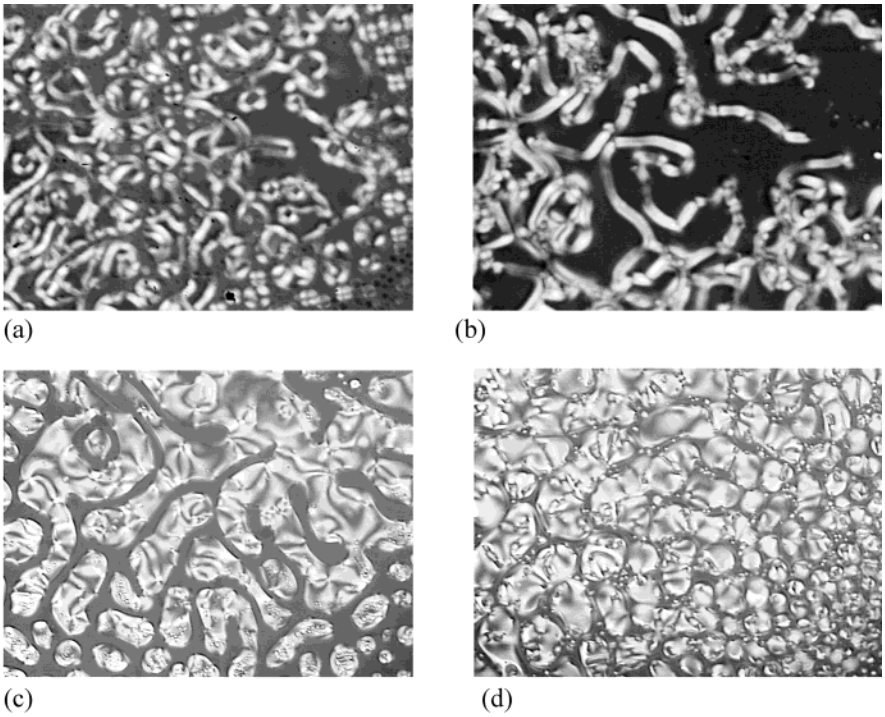

Figure 2. Photomicrographs of supramolecular liquid crystals: (a) complex $\mathbf{1}_{0.9}/\mathbf{5}_{0.1}/\mathbf{6}$ at 165 °C, cooling; (b) complex $\mathbf{1}_{0.75}/\mathbf{5}_{0.25}/\mathbf{6}$ at 166 °C, cooling; (c) complex $\mathbf{2}_{0.9}/\mathbf{5}_{0.1}/\mathbf{6}$ at 193 °C, cooling; and (d) complex $\mathbf{2}_{0.75}/\mathbf{5}_{0.25}/\mathbf{6}$ at 190 °C, cooling.

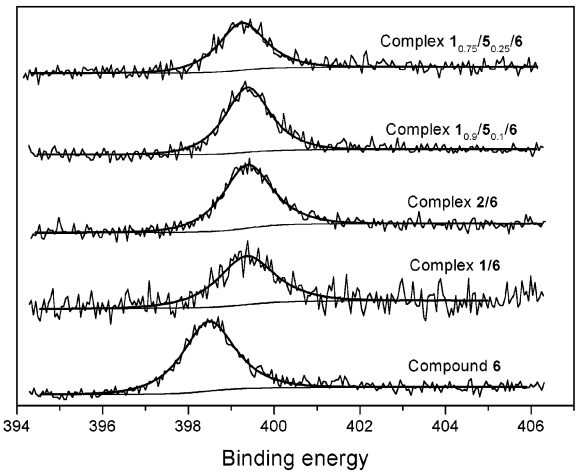

Figure 3. N 1s core-level spectra of compound **6** and complexes.

a delocalization of electronic charge, which results in a net decrease in electron density at both donor and acceptor; consequently, it is possible to detect the chemical shift change of nuclei that are involved in the formation of the hydrogen bond. The N 1s spectra of complexes **1**/**6**, **2**/**6**, $\mathbf{1}_{0.9}/\mathbf{5}_{0.1}/\mathbf{6}$, $\mathbf{1}_{0.75}/\mathbf{5}_{0.25}/\mathbf{6}$, and acceptor **6** are shown in Figure 3. The N 1s spectra were deconvoluted by employing a combination of Gaussian (80%) and Lorentz (20%) methods. The shifts of binding energy of N 1s and carbonyl C 1s are also summarized in Table 2. The binding energy shift is frequently used to distinguish whether the hydrogen-bonding or ionic interaction between the donor and acceptor is formed. It is also indicative in evaluating the strength of the hydrogen bond. In the N 1s spectrum of compound **6,** a peak emerged at 398.49 eV; however, all N 1s spectra of complexes exhibited a peak with a larger binding energy relative to the free acceptor **6**. No distinct shoulder or significant broadening peak was observed in the spectra of complexes, so it is difficult to deconvolute the nonassociated N 1s from the composite N 1s peak. This seems to indicate that majority of donors take part in the formation of the hydrogen bond in solid state. The changes in N 1s binding energy are in the range from 0.77 to 0.89 eV. If the hydrogen-bonding interaction is associated, the difference of the N 1s binding energy between the free **6** and complexed **6** should be less than 1.0 eV.[29] Therefore, we can conclude that no ionic interaction was present in the complexes we studied. It was also observed that there is no considerable difference between the binary and ternary complexes for the N 1s binding energy, implying that both binary and ternary complexes have the same characteristics of the hydrogen bonding. The carbonyl C 1s gave somewhat information, although it is not so sensitive as the N 1s. The binding energy of the carbonyl C 1s decreased by 0.18−0.40 eV relative to the free diacids, which is less than the change of the N 1s binding energy as expected. The change in binding energy of the carbonyl C 1s is in fact consistent with the change in electronic density due to the formation of the hydrogen bond. The formation of the hydrogen bond (O═C−O−H···N) by dissociating acid dimer would allow carbonyl oxygen atom not to be involved in the hydrogen bond in the complexes (Figure 4). This simultaneously

Table 2. Binding Energy and Shift of N 1s and C 1s(C═O) in Supramolecular Complexes[a]

complex	N 1s (eV)	shift[b] (eV)	C 1s (eV) (C═O)	shift[b] (eV)
1/**6**	399.36	0.87	289.09	−0.18
2/**6**	399.38	0.89	289.06	−0.21
3/**6**	399.22	0.73	288.88	−0.39
$\mathbf{1}_{0.9}/\mathbf{5}_{0.1}/\mathbf{6}$	399.38	0.89	288.87	−0.40
$\mathbf{1}_{0.75}/\mathbf{5}_{0.25}/\mathbf{6}$	399.26	0.77	288.99	−0.28

[a] All core-level spectra were referenced to the C 1s neutral carbon peak at a binding energy (BE) of 285 eV in order to compensate for surface charge effects. [b] Shift = $BE_{SC} - BE_A$ (or BE_D), where BE_{SC}, BE_A, and BE_D represent the binding energy of supramolecular complex, acceptor (398.49 eV), and donor (289.27 eV), respectively.

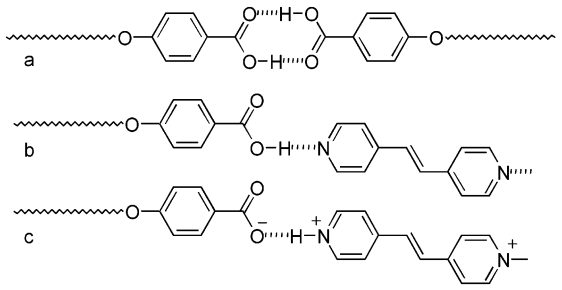

Figure 4. Schematic representation of donor associate and complexes: (a) donor dimer, (b) donor−acceptor molecular complex, and (c) donor−acceptor zwitterionic complex.

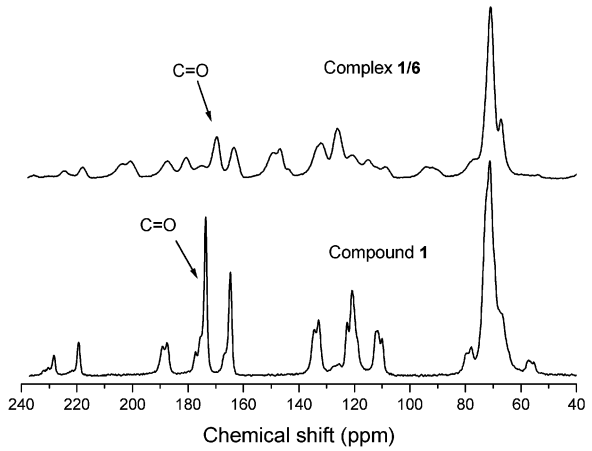

Figure 5. Solid-state CP/MAS ^{13}C NMR spectra of semicrystalline complex **1**/**6** and compound **1** at 298 K.

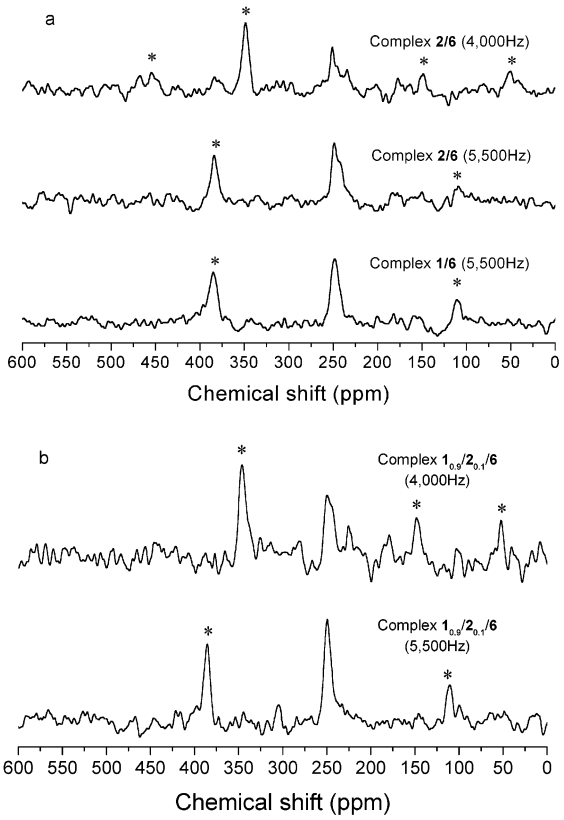

Figure 6. Solid-state CP/MAS ^{15}N NMR spectra of (a) semicrystalline complexes **1**/**6**, **2**/**6** and (b) $\mathbf{1}_{0.9}$/$\mathbf{5}_{0.1}$/**6** at 298 K. "*" denotes the spinning sidebands.

brought about an increase of the electronic density of the carbonyl carbon, thus leading to a decrease of the binding energy of the carbonyl C 1s.

Solid-State NMR Characterization. As mentioned above, these supramolecular complexes exhibit liquid crystal behaviors at higher temperature, while at the room temperature they form semicrystalline polymers held by hydrogen bonds. The solid-state ^{13}C NMR spectra of semicrystalline complexes **1**/**6** and **2**/**6** together with donors **1** and **2** were determined at 298 K. The spectra of complex **1**/**6** and compound **1** are shown in Figure 5. The chemical shifts of carbonyl carbon for free donors **1** and **2** are at 173.6 and 173.4 ppm, respectively, whereas the chemical shifts of carbonyl carbon move to 169.6 and 167.8 ppm, respectively, for complexes **1**/**6** and **2**/**6**. Similar to XPS, the NMR chemical shift of an atom is dependent on its electronic and molecular environments. For acid dimer, both oxygen atoms in the carboxylic acid participate in the formation of strong hydrogen bonds, but only one oxygen atom from the hydroxy group is involved in the hydrogen bond when a complex is formed (Figure 4). This would increase the electron density at the carbonyl carbon of the complexes in comparison with the acid dimer and thus induce an upfield shift for carbonyl carbon ($\Delta\delta$ = 4.0 and 5.6 ppm).

It is of significance to study the ^{15}N NMR spectra of the complexes because nitrogen serves directly as a proton acceptor. The solid-state natural abundance CP/MAS ^{15}N NMR spectra of semicrystalline complexes **1**/**6**, **2**/**6**, and $\mathbf{1}_{0.9}$ /$\mathbf{5}_{0.1}$/**6** were determined at 298 K and are given in Figure 6. Spinning sidebands were located by changing the spinning frequency of the sample. In ^{15}N NMR spectra, signals appeared at 248.3, 248.9, and 249.6 ppm for complexes **1**/**6**, **2**/**6**, and $\mathbf{1}_{0.9}$ /$\mathbf{5}_{0.1}$/**6**, respectively. No unassociated ^{15}N signal was observed in the spectra. As can be clearly seen in Figure 6, all complexes have almost the same ^{15}N chemical shift, irrespective of composition of the complexes. This suggests that incorporation of the third component **5** does not significantly affect the ^{15}N chemical shift of **6**. In the D−A complexes ^{15}N chemical shift depends on the nitrogen−hydrogen distance, and this correlation can be used to evaluate hydrogen bond geometry.[19] In comparison with the free **6**, the ^{15}N chemical shift of compound **6** in the complexes is estimated to be an upfield shift of ca. 29 ppm.[18,30] This upfield shift is close to that of collidine and benzoic acid complex ($\Delta\delta$ = 34 ppm) but much less than that of the zwitterionic structures (ionic interaction) formed by pyridine and mineral acid ($\Delta\delta \geq$ 105 ppm).[18,19] It indicates that the complexes **1**/**6**, **2**/**6**, and $\mathbf{1}_{0.9}$ /$\mathbf{5}_{0.1}$/**6** have the nature of molecular complexes which have typical hydrogen-bonding characteristics. The hydrogen bond proton is closer to oxygen than nitrogen, and no zwitterionic structure is formed as shown in Figure 4b.

Conclusions

The hydrogen-bonded supramolecular complexes were synthesized by complementary self-assembly. An additional proton donor **5** was included in the complexes and consequently reduced the relative order of self-assembly. Only less ordered nematic phases were observed in the ternary complexes, being different from the binary complexes that showed a smectic phase. A tetrafunctional proton donor was used to prepare the complex; however, no liquid crystallinity was observed. An XPS investigation illustrated that both binary and

ternary complexes have characteristics of hydrogen-bonded molecular complexes rather than zwitterionic complexes in terms of the binding energy change of N 1s. Observation of solid-state CP/MAS ^{13}C NMR and ^{15}N NMR also supported the XPS results.

Acknowledgment. We gratefully acknowledge the financial support from Institute of Materials Research and Engineering.

References and Notes

(1) Paleos, C. M.; Tsiourvas, D. *Liq. Cryst.* **2001**, *28*, 1127 and references therein.
(2) Paleos, C. M.; Tsiourvas, D. *Angew. Chem., Int. Ed. Engl.* **1995**, *34*, 1696.
(3) Kato, T. In *Handbook of Liquid Crystals*; Demus, D., Goodby, J., Gray, G. W., Spiess, H. W., Vill, V., Eds.; Wiley-VCH: Weinheim, 1998; pp 969−979. (b) Blunk, D.; Praefcke, K.; Vill, V. In *Handbook of Liquid Crystals*; Demus, D., Goodby, J., Gray, G. W., Spiess, H. W., Vill, V., Eds.; Wiley-VCH: Weinheim, 1998; pp 305−340.
(4) Lu, X. H.; He, C. B.; Terrell, C. D.; Griffin, A. C. *Macromol. Chem. Phys.* **2002**, *203*, 85.
(5) Kato, T.; Mizoshita, N.; Kanie, K. *Macromol. Rapid Commun.* **2001**, *22*, 797.
(6) Prins, L. J.; Reinhoudt, D. N.; Timmerman, P. *Angew. Chem., Int. Ed.* **2001**, *40*, 2382.
(7) Kato, T.; Nakano, M.; Moteki, T.; Uryu, T.; Ujiie, S. *Macromolecules* **1995**, *28*, 8875.
(8) Kato, T.; Fréchet, J. M. J. *Macromol. Symp.* **1995**, *98*, 311.
(9) Kato, T.; Fréchet, J. M. J. *J. Am. Chem. Soc.* **1989**, *111*, 8533.
(10) Kato, T.; Fréchet, J. M. J. *Macromolecules* **1989**, *22*, 3818.
(11) Kihara, H.; Kato, T.; Uryu, T.; Fréchet, J. M. J. *Chem. Mater.* **1996**, *8*, 961.
(12) Pourcain, C. B. S.; Griffin, A. C. *Macromolecules* **1995**, *28*, 4116.
(13) Bladon, P.; Griffin, A. C. *Macromolecules* **1993**, *26*, 6604.
(14) He, C. B.; Donald, A. M.; Griffin, A. C.; Waigh, T.; Windle, A. H. *J. Polym. Sci., Polym. Phys. Ed.* **1998**, *36*, 1617.
(15) Lee, C.-M.; Griffin, A. C. *Macromol. Symp.* **1997**, *117*, 281.
(16) Lee, M.; Cho, B. K.; Kang, Y. S.; Zin, W. C. *Macromolecules* **1999**, *32*, 8531.
(17) Kumar, U.; Kato, T.; Fréchet, J. M. J. *J. Am. Chem. Soc.* **1992**, *114*, 6630.
(18) Solum, M. S.; Altmann, K. L.; Strohmeier, M.; Berges, D. A.; Zhang, Y.; Facelli, J. C.; Pugmire, R. J.; Grant, D. M. *J. Am. Chem. Soc.* **1997**, *119*, 9804.
(19) Lorente, P.; Shenderovich, I. G.; Golubev, N. S.; Denisov, G. S.; Buntkowsky, G.; Limbach, H.-H. *Magn. Reson. Chem.* **2001**, *39*, S18−S29.
(20) Smirnov, S. N.; Golubev, N. S.; Denisov, G. S.; Benedict, H.; Schah-Mohammedi, P.; Limbach, H.-H. *J. Am. Chem. Soc.* **1996**, *118*, 4094.
(21) Luo, X. F.; Goh, S. H.; Lee, S. Y.; Huan, Cha. *Macromol. Chem. Phys.* **1999**, *200*, 874.
(22) Goh, S. H.; Lee, S. Y.; Dai, J.; Tan, K. L. *Polymer* **1996**, *37*, 5305.
(23) Zhou, X.; Goh, S. H.; Lee, S. Y.; Tan, K. L. *Appl. Surf. Sci.* **1998**, *126*, 141.
(24) Zhou, X.; Goh, S. H.; Lee, S. Y.; Tan, K. L. *Polymer* **1998**, *39*, 3631.
(25) Luo, X. F.; Goh, S. H.; Lee, S. Y.; Tan, K. L. *Macromolecules* **1998**, *31*, 3251.
(26) Wilson, L. M. *Liq. Cryst.* **1995**, *18*, 381.
(27) Alexander, C.; Jariwala, C. P.; Lee, C.-M.; Griffin, A. C. *Macromol. Symp.* **1994**, *77*, 283.
(28) Lee, C.-M.; Jariwala, C. P.; Griffin, A. C. *Polymer* **1994**, *35*, 4550.
(29) Li, X.; Goh, S. H.; Lai, Y. H.; Wee, A. T. S. *Polymer* **2001**, *42*, 5463.
(30) The ^{15}N chemical shifts of bipyridyl ethylene (279 ppm) was estimated based on the chemical shift of pyridine and was converted into the solid ^{15}N glycine scale.

MA020971U